Research Article

Ziru Li, Jiaqi Zhao, Meiqi Lou, and Xiuyan Wang*

Synthesis and structural characterization of a novel lead coordination polymer: $[Pb(L)(1,3\text{-bdc})]\cdot 2H_2O$

https://doi.org/10.1515/mgmc-2022-0021
received June 28, 2022; accepted August 17, 2022

Abstract: A novel coordination polymer, $[Pb(L)(1,3\text{-bdc})]\cdot 2H_2O$ (**1**), (L = 2-(2,6-dichlorophenyl)-1*H*-imidazo[4,5-*f*][1,10]phenanthroline, 1,3-H_2bdc = 1,3-benzenedicarboxylic acid) has been successfully prepared under hydrothermal conditions. The structure of **1** is a 1D chain structure, which further stacks together to form a 3D supramolecular architecture by π–π interactions and C–H···π interactions. In addition, the thermogravimetric analysis of **1** has been investigated.

Keywords: lead(II), coordination polymer, crystal structure, 1,10-phenanthroline derivate

1 Introduction

Recently, coordination polymers have attracted great interest for their unique structural diversities and potential applications (Lu et al., 2020; Zhao et al., 2022) such as catalysis (Wang et al., 2017), gas storage (Gándara et al., 2014), fluorescent probes (Wang., 2019; Lin et al., 2016; Li et al., 2020), magnetism (Deng et al., 2019; Jankowski et al., 2019), biological uses (Raja et al., 2012), and so on. The process of coordination polymers' self-assembly is also affected by many factors, such as the choosing of metal center and nitrogen-containing ligand, pH value, mole ratio, solvent, and so on, as any small difference may result in a different final structure of the product than the original target structure (Bharati et al., 2020; Li et al., 2021b; Yang et al., 2021; Yu et al., 2020). Nitrogen-containing ligand is a kind of excellent ligand widely used as bridging and chelating blocks to construct coordination polymers (Li et al., 2021a,c; Tian et al., 2016; Wu et al., 2016; Xu et al., 2007). In this regard, phenanthroline derivatives, a rigid nitrogen-containing ligand, can promote charge transfer and stabilize the coordination polymers (Xu et al., 2022; Zhang et al., 2003). To our knowledge, reports on the coordination polymers based on the 2-(2,6-dichlorophenyl)-1*H*-imidazo[4,5-*f*][1,10]phenanthroline are very limited (Wang et al., 2015).

With the aforementioned considerations, we selected 2-(2,6-dichlorophenyl)-1*H*-imidazo[4,5-*f*][1,10]phenanthroline (L) as a nitrogen-containing ligand and 1,3-benzenedicarboxylic acid (1,3-H_2bdc) as a connector to construct a new coordination polymer $[Pb(L)(1,3\text{-bdc})]\cdot 2H_2O$.

2 Results and discussion

2.1 Structural analysis

The asymmetric unit of **1** consists of one unique Pb(II) atom, one L ligand, one 1,3-bdc anion, and two free water molecules. As shown in Figure 1, the coordination environment of atom Pb(II) is completed by four carboxylate oxygen atoms (O(1), O(2), O(3^{iii}), and O(4^{iii})) from two different 1,3-bdc anions and one nitrogen atom (N(2)) from one chelating L ligand in the equatorial plane, and one N atom (N(1)) in vertex positions. The Pb–O and Pb–N distances in **1** are comparable to those reported in other analogous complex $[Pb(L)(adip)_{0.5}]$ (H_2adip = adipic acid, HL = 1-(1*H*-imidazo[4,5-*f*][1,10]phenanthrolin-2-yl) naphthalen-2-ol) (Table 1) (Song et al., 2021). The 1,3-bdc anions link two neighboring Pb(II) atoms in a bis-chelating

* **Corresponding author: Xiuyan Wang,** Key Laboratory of Preparation and Applications of Environmental Friendly Materials, Jilin Normal University, Ministry of Education, Changchun 130103, China; Department of Chemistry, Jilin Normal University, Siping 136000, China, e-mail: wangxiuyanjlnu2004@163.com
Ziru Li: Key Laboratory of Preparation and Applications of Environmental Friendly Materials, Jilin Normal University, Ministry of Education, Changchun 130103, China; Department of Chemistry, Jilin Normal University, Siping 136000, China
Jiaqi Zhao, Meiqi Lou: Department of Chemistry, Jilin Normal University, Siping 136000, China

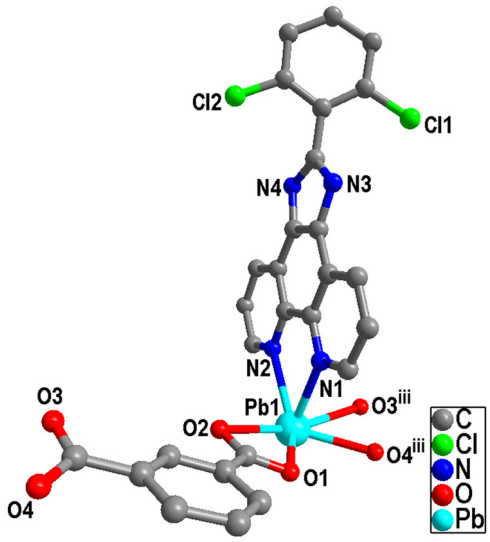

Figure 1: View of the coordination environment of the **Pb**(II) atom in **1** (symmetric codes: [iii]x–1/2, y + 1/2, z).

Table 1: Selected bond lengths (Å) and angles (°) for the complex **1**

Pb(1)–N(1)	2.492(6)
Pb(1)–N(2)	2.630(6)
Pb(1)–O(1)	2.494(6)
Pb(1)–O(2)	2.708(6)
Pb(1)–O(3)[i]	2.613(5)
Pb(1)–O(4)[i]	2.441(7)
O(4)–Pb(1)–N(1)[ii]	80.0(2)
O(4)–Pb(1)–O(1)[ii]	78.11(18)
N(1)–Pb(1)–O(1)	78.8(2)
O(4)–Pb(1)–O(3)[ii]	51.55(19)
N(1)–Pb(1)–O(3)[ii]	83.6(2)
O(1)–Pb(1)–O(3)[ii]	128.8(2)
O(4)–Pb(1)–N(2)[ii]	120.34(19)
N(1)–Pb(1)–N(2)	64.8(2)
O(1)–Pb(1)–N(2)	133.15(18)
O(3)–Pb(1)–N(2)[ii]	76.93(18)
O(4)–Pb(1)–O(2)[ii]	126.62(19)
N(1)–Pb(1)–O(2)	79.2(2)
O(1)–Pb(1)–O(2)	49.85(18)
O(3)–Pb(1)–O(2)[ii]	162.6(2)
N(2)–Pb(1)–O(2)	93.30(19)

Symmetry codes: [i]x–1/2, y + 1/2, z; [ii]x + 1/2, y–1/2, z.

mode to generate a one-dimensional chain with the Pb···Pb separation of 10.217 Å (Figure 2). Moreover, the 1,3-bdc anions are stacked with those of an adjacent chain through π–π interactions to form a one-dimensional double-chain structure (centroid-to-centroid distance 3.604(4) Å and face-to-face distance 3.487(3) Å, and dihedral angle of 0.0(4)°) (Figure 3).

Interestingly, as shown in Figure 4, other π–π interactions have been observed in **1**, and the L ligands from the double chains furnish π–π stacking interactions between the L ligands of neighboring chains [N(1)/C(1)–C(5), N(2)/C(6)–C(10) at (x, −1 + y, z), centroid-to-centroid distance of 3.642(4) Å and face-to-face distance of 3.248(3) Å, and dihedral angle of 1.6(4)°], resulting in a two-dimensional supramolecular layer (Figure 5). More interestingly, the C–H···π interactions have also been found in **1**. It is the C–H···π interactions between the C(17) atom of the L ligand and the benzene ring [C(21)–C(26) at (−x, y, 1/2−z)] of 1,3-bdc anion (2.94 Å, and angle of 12.23°) (Figure 6), which make the two-dimensional layers to generate a three-dimensional supramolecular architecture (Figure 7).

2.2 PXRD pattern and thermal analysis

To check the relative purity of **1**, the powder X-ray diffraction patterns were carried out for **1**. The experimental powder X-ray diffraction patterns of **1** match well with the corresponding simulated patterns obtained from the single crystal data, thus proving the phase purity of the synthesized samples (Figure 8).

To study the stability of **1**, thermogravimetric analysis (TGA) was performed. As shown in Figure 9, the TG curve reveals that the first weight loss of 4.6% between 53°C and 174°C corresponds to the loss of the two free water molecules (calcd. 4.7%). The second weight loss from 219°C to 552°C can be attributed to the decomposition of the organic group $C_8H_4O_3$ of 1,3-bdc anion and L ligand

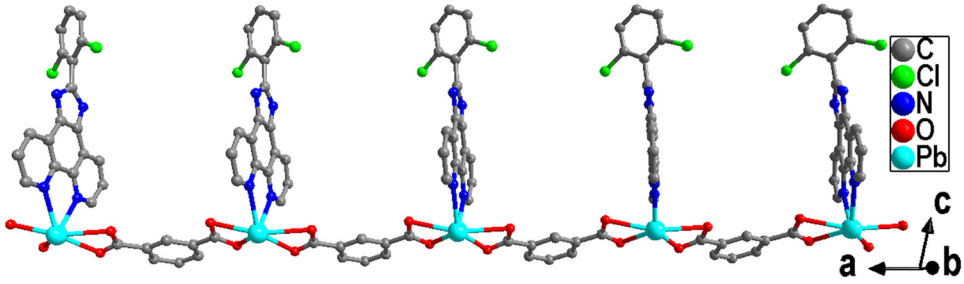

Figure 2: View of the 1D chain of **1** constructed by the 1,3-bdc.

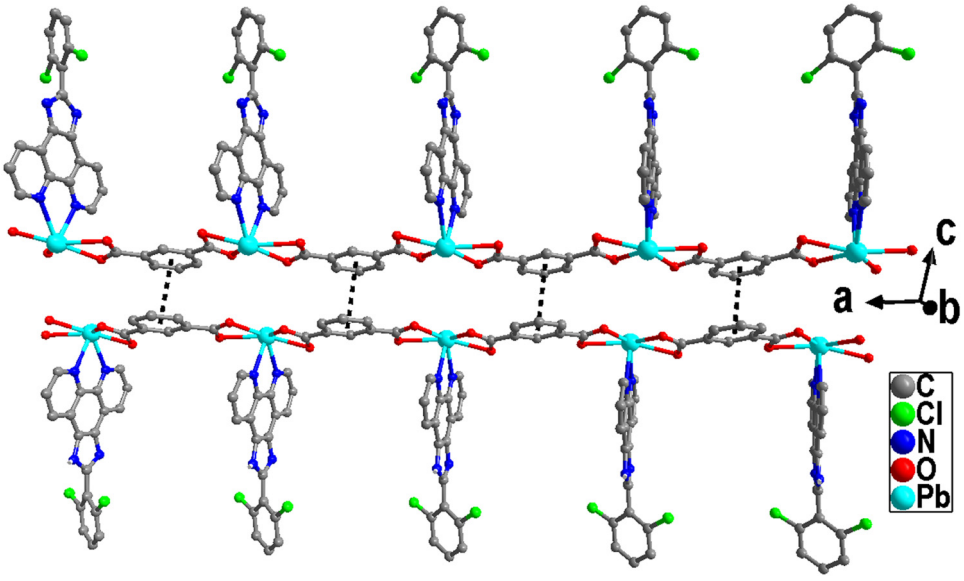

Figure 3: View of the 1D double-chain structure of **1** formed by π–π interactions.

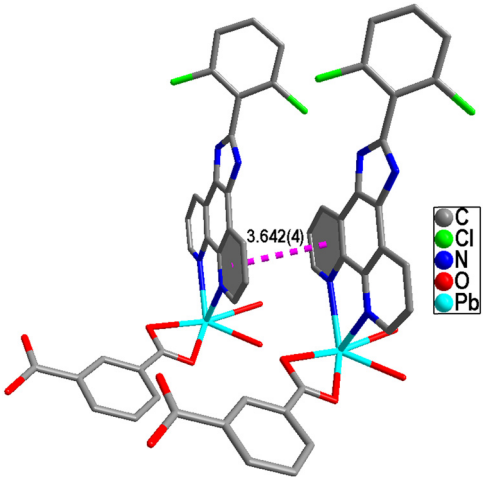

Figure 4: View of the π–π interactions in **1**.

(weight loss: 66.3%; calcd. 66.4%). The TGA results basically agree with the formula of the title complex.

3 Conclusions

A Pb(II) coordination polymer [Pb(L)(1,3-bdc)]·2H_2O (**1**) has been synthesized under hydrothermal conditions with the mixed ligands of the 1,3-benzenedicarboxylic acid (1,3-H_2bdc) and 2-(2,6-dichlorophenyl)-1*H*-imidazo[4,5-*f*][1,10]phenanthroline (L). The 1,3-bdc anions link two neighboring Pb(II) atoms to acquire a one-dimensional (1D) chain. The aforementioned 1D chains generate further a two-dimensional (2D) supramolecular layer by two kinds of π–π aromatic packing interactions. The 2D

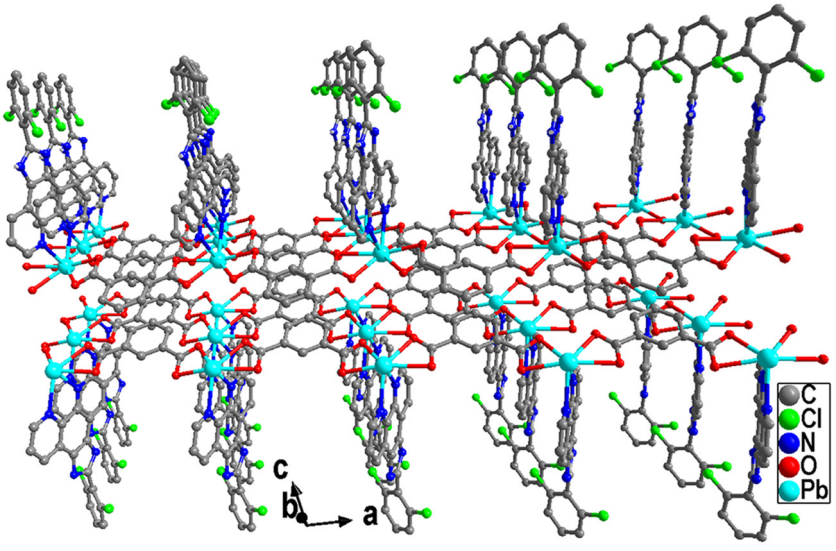

Figure 5: View of the 2D supramolecular structure of **1** formed by the other π–π interactions.

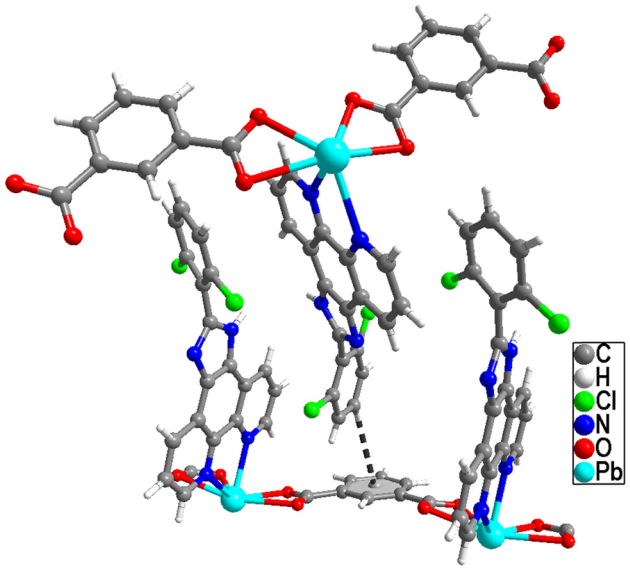

Figure 6: View of the C–H···π interactions in **1**.

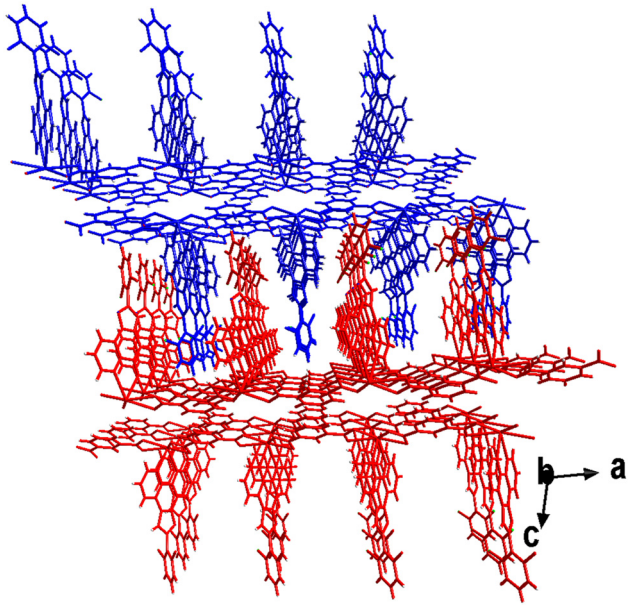

Figure 7: View of the 3D supramolecular structure of **1** formed by C–H···π interactions.

supramolecular layers are extended into a three-dimensional (3D) supramolecular architecture via C–H···π interactions. Moreover, the powder X-ray diffraction patterns and thermogravimetric analysis of 1 have been studied.

Experimental

All reagents and solvents for syntheses were bought from the commercial companies (Jinan Henghua Sci. &

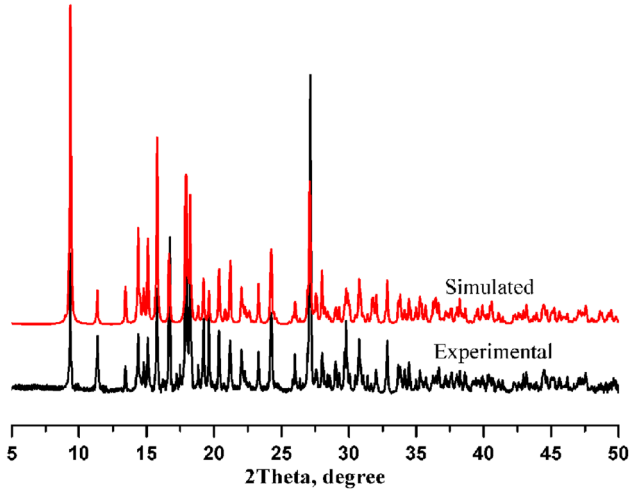

Figure 8: View of the powder X-ray diffraction patterns of **1**.

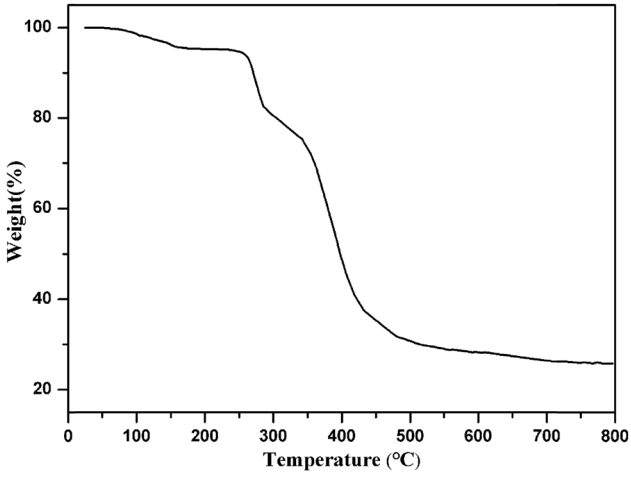

Figure 9: View of the thermal analysis curve of **1**.

Tec. Co. Ltd and Jiangsu Hengxiang Chemical Sales Co. Ltd, China). Thermogravimetric analyses (TGA) were performed on a TG SDT2960 thermal analyzer under nitrogen gas (TA, USA). Powder X-ray diffraction (PXRD) patterns were measured on a Rigaku Dmax 2000 X-ray diffractometer with graphite-monochromatized CuKα radiation (Rigaku, Japan). Elemental analyses for C, H, and N were performed on a Perkin-Elmer 240 CHN elemental analyzer (Perkin Elmer, North Waltham, USA).

Preparation of [Pb(L)(1,3-bdc)]·2H_2O (1)

A mixture of $Pb(NO_3)_2$ (0.4 mmol, 0.132 g), L (0.4 mmol, 0.146 g), 1,3-H_2bdc (0.4 mmol, 0.066 g), and H_2O (9 mL) was adjusted to the pH value to 7.03 with triethylamine.

The mixture was stirred for 30 min at room temperature, then transferred to a 20 mL Teflon reaction kettle and heated at 160°C for 96 h, and then cooled to room temperature at rate of 5°C·h^{-1}. The yellow block-shaped crystals of **1** were obtained in 45% yield (based on the Pb). Analytical found for $C_{27}H_{18}Cl_2N_4O_6Pb$, calcd. %: C, 41.97; H, 2.35; N, 7.25; found %: C, 40.46; H, 2.31; N, 7.16. Selected IR (KBr) cm^{-1}: 3,416 [ν(H$_2$O)], 1,580 [ν_{as}(COO)], 1,414 [ν_s(COO)], 1,329, 1,240, 1,075 [ν(C═N)], 897, 813, 735, 640, 557.

X-ray crystallography

The single-crystal diffraction data for **1** were collected on a Bruker-AXS Smart CCD diffractometer with graphite-monochromatized Mo-Kα radiation (λ = 0.71073 Å) by ϕ and ω scan mode at 298 (2) K. All of the structures were solved by direct methods using SIR2014 (Burla et al., 2015) and refined by full-matrix least-squares methods based on F2 using SHELXL2018/3 program (Sheldrick, 2015). All the nonhydrogen atoms were located directly and refined anisotropically. The hydrogen atoms attached to carbon atoms were set in the calculated positions and refined as a riding model. Detailed crystal data and structure refinement are listed in Table 2. The selected bond lengths and angles are listed in Table 1. Crystallographic data have been deposited with the Cambridge Crystallographic Data Centre as supplementary publication numbers CCDC 2182312. The Cambridge Crystallographic Data Centre via www.ccdc.cam.ac.uk/data_request/cif.

Table 2: Crystalline data and refinement parameters for complex **1**

Empirical formula	$C_{27}H_{18}Cl_2N_4O_6Pb$
Formula weight	772.54
Crystal system	Monoclinic
Space group	*C*2/*c*
a (Å)	19.4331(18)
b (Å)	6.3184(6)
c (Å)	40.553(4)
β (°)	103.2850(10)
Volume (Å^3)	4,846.1(8)
Z	8
D_c (g·cm^{-3})	2.118
μ (mm^{-1})	7.239
F(000)	2,976
θ range (°)	2.154–25.006
Crystal size (mm)	0.218 × 0.191 × 0.152
Tot. reflections	4,254
Uniq. reflections, R_{int}	13,415, 0.0220
GOF on F^2	1.107
R_1 indices [$I > 2\sigma(I)$]	0.0446
wR_2 indices (all data)	0.1054
$\Delta\rho_{min}$, $\Delta\rho_{max}$ (e·Å^{-3})	−2.672, 1.510
CCDC No.	2182312

Funding information: This work was supported by the Science and Technology Development Program of Jilin Province (YDZJ202201ZYTS595) and the Graduate Innovation Project of Jilin Normal University (No. 202030).

Author contributions: Ziru Li: writing – original draft, experimental work; Jiaqi Zhao: writing – original draft, data curation, visualization; Meiqi Lou: experimental work, software; Xiuyan Wang: writing – review and editing, validation, supervision.

Conflict of interest: The authors state no conflict of interest.

Data availability statement: All data generated or analyzed during this study are included in this published article.

References

Bharati A.K., Somnath., Lama P., Siddiqui K.A., A novel mixed ligand Zn-coordination polymer: synthesis, crystal structure, thermogravimetric analysis and photoluminescent properties. *Inorg Chim Acta*., 2020, 500, 119219. doi: 10.1016/j.ica.2019.119219.

Burla M.C., Caliandro R., Carrozzini B., Cascarano G.L., Cuocci C., Giacovazzo C., et al., Crystal structure determination and refinement via SIR2014. *J. Appl. Cryst.*, 2015, 48, 306–309. doi: 10.1107/S1600576715001132.

Deng Q.J., Wang H.L., Zhu Z.H., Ma X.F., Huang K.Z., Huang M.L., et al. Stepwise fragmentation of asymmetric triangular shape Ln3 cluster and magnetocaloric effect of Gd3 analogue. *J Clust Sci*., 2019, 30, 1171–1176. doi: 10.1007/s10876-019-01495-x.

Gándara F., Furukawa H., Lee S., Yaghi O.M., High methane storage capacity in aluminum metal-organic frameworks. *J Am Chem Soc*., 2014, 136(14), 5271–5274. doi: 10.1021/ja501606h.

Jankowski R., Zakrzewski J.J., Surma O., Ohkoshi S.i., Chorazy S., Sieklucka B., Near-infrared emissive Er(III) and Yb(III) molecular nanomagnets in metal-organic chains functionalized by octacyanidometallates(IV). *Inorg Chem Front*., 2019, 6(9), 2423–2434. doi: 10.1039/C9QI00583H.

Lin H.Y., Rong X., Liu G.C., Wang X., Wang X.L., Duan S.R., Fluorescent sensing and electrocatalytic properties of three Zn(II)/Co(II) coordination complexes containing two different dicarboxylates and two various bis(pyridyl)-bis(amide) ligands. *J Mol Struct*., 2016, 1119, 396–403. doi: 10.1016/j.molstruc.2016.04.085.

Li J.X., Du Z.X., Xiong L.Y., Fu L.L., Bo W.B., Supramolecular isomerism in two nickel(II) coordination polymers constructed

with the flexible 2-carboxyphenoxyacetate linker: Syntheses, structure analyses and magnetic properties. *J Solid State Chem*., 2021a, 293, 121799. doi: 10.1016/j.jssc.2020.121799.

Li N.Y., Chen J.M., Tang X.Y., Zhang G.P., Liu D., Reversible single-crystal-to-single-crystal conversion of a photoreactive coordination network for rewritable optical memory storage. *Chem Commun*., 2020, 56, 1984–1987. doi: 10.1039/C9CC09081A.

Li N.Y., Jiang Z.D., Wang Y. J., Liu L.L., Liu D., Crystallographic visualization of a guest-induced solar-driven cycloaddition reaction based on a recyclable nonporous coordination polymer. *Inorg Chem*., 2021b, 60(22), 17173–17177. doi: 10.1021/acs.inorgchem.1c02477.

Li Y., Yang J., Ma J.F., A copper(II)-based porous metal-organic framework for the efficient and rapid capture of toxic oxo-anion pollutants from water. *Dalton T*., 2021c, 50(11), 3832–3840. doi: 10.1039/d0dt04252h.

Lu Z.Y., Liu J., Zhang X., Liao Y.Z., Wang R., Zhang K., et al., Node-Accessible Zirconium MOFs. *J Am Chem Soc*., 2020, 142(50), 21110–21121. doi: 10.1021/jacs.0c09782.

Raja D.S., Bhuvanesh N.S.P., Natarajan K., A novel water soluble ligand bridged cobalt(II) coordination polymer of 2-oxo-1,2-dihydroquinoline-3-carbaldehyde (isonicotinic) hydrazone: evaluation of the DNA binding, protein interaction, radical scavenging and anticancer activity. *Dalton T*., 2012, 41(15), 4365–4377. doi: 10.1039/c2dt12274j.

Sheldrick G.M., Crystal structure refinement with SHELXL. *Acta Cryst*., 2015, C71, 3–8. doi: 10.1107/S2053229614024218.

Song Y., Yan Y., Zhang H., Wang X.Y., Synthesis and structural characterization of a novel 2D supramolecular lead coordination polymer with phenanthroline derivate and adipic acid. *Main Group Met. Chem*., 2021, 44, 239–242. doi: 10.1515/mgmc-2021-0025.

Tian A.X., Ji X.B., Sun N., Xiao R., Zhao Y.Y., Ni H.P., et al., Four new coordination polymers constructed by 2-(4-Thiazolyl)benzimidazole and 1,3,5-benzenetricarboxylic acid. *J Chem Crystallogr*., 2016, 47(1–2), 1–9. doi: 10.1007/s10870-016-0674-7.

Wang L., A dual-functional Lead(II) metal-organic framework based on 5-aminonicotinic acid as a luminescent sensor for selective sensing of nitroaromatic compounds and detecting the temperature. *J Inorg Organomet P*., 2019, 30(2), 291–298. doi: 10.1007/s10904-019-01186-0.

Wang X.L., Sun J.J., Lin H.Y., Chang Z.H., Liu G.C., Wang X., A series of novel anderson-type polyoxometalate-based Mn(II) complexes constructed from pyridyl-derivatives: assembly, structures, electrochemical and photocatalytic properties. *CrystEngComm*., 2017, 19(23), 3167–3177. doi: 10.1039/C7CE00659D.

Wang Y.W., Zhang Y., Zhu D., Ma K., Ni H., Tang G., Synthesis, structural characterization and theoretical approach of the tri(2-(2,6-dichlorophenyl)-1*H*-imidazo[4,5-*f*][1,10]phenanthroline) cobalt(II). *Spectrochim Acta A*., 2015, 147, 31–42. doi: 10.1016/j.saa.2015.02.053.

Wu Z.B., Yuan X.Z., Zhang J., Wang H., Jiang L.B., Zeng G.M., Photocatalytic decontamination of wastewater containing organic dyes by metal-organic frameworks and their derivatives. *ChemCatChem*., 2016, 9(1), 41–64. doi: 10.1002/cctc.201600808

Xu N., Cui M.H., Zhang Y.Y., Chang L.M., Kong Z.G., Xu Z.L., Synthesis and crystal structure of one new cadmium coordination polymer constructed by phenanthroline derivate and 1,4-naphthalenedicarboxylic acid. *Main Group Met Chem*., 2022, 45(1), 86–91. doi: 10.1515/mgmc-2022-0005.

Xu X.H., Lin H., Lin H.K., Trinuclear metal complexes based on 1,10-phenanthroline derivates as catalysts for cleavage of a RNA-model substrate. *Chem Res in Chinese U.*, 2007, 23(5), 493–499. doi: 10.1016/s1005-9040(07)60107-x.

Yang F., Li N.Y., Ge Y., Liu D., Single-crystal to single-crystal transformation of a coordination chain to a two-dimensional coordination network through a photocycloaddition reaction. *CrystEngComm*., 2021, 23, 2783–2787. doi: 10.1039/D1CE00230A.

Yu C.X., Wang K.Z., Li X.J., Liu D., Ma L.F., Liu L.L., Highly efficient and facile removal of Pb^{2+} from water by using a negatively charged azoxy-functionalized metal-organic framework. *Cryst Growth Des*., 2020, 20(8), 5251–5260. doi: 10.1021/acs.cgd.0c00437.

Zhang L.P., Wan Y.H., Jin L.P., Hydrothermal synthesis and crystal structure of neodymium(III) coordination polymers with isophthalic acid and 1,10-phenanthroline. *Polyhedron*., 2003, 22, 981–987. doi: 10.1016/S0277-5387(03)00021-4.

Zhao P.R., Liu Y.Q., He C., Duan C.Y., Synthesis of a lanthanide metal-organic framework and its fluorescent detection for phosphate group-based molecules such as adenosine triphosphate. *Inorg. Chem*., 2022, 61(7), 3132–3140. doi: 10.1021/acs.inorgchem.1c03412.